Counterion-induced processibility of polyaniline: Transport at the metal-insulator boundary

M. Reghu, Y. Cao, D. Moses, and A. J. Heeger

Institute for Polymers and Organic Solids, University of California, Santa Barbara, California 93106

(Received 12 June 1992; revised manuscript received 26 October 1992)

Polyaniline (PANI) films of superior homogeneity can be prepared by using functionalized protonic acids to protonate the polymer and simultaneously induce solubility, *in the conducting form*, in common organic solvents. The results of measurements of the temperature dependence and magnetic-field dependence of the conductivity of films of PANI complexed with camphor sulfonic acid (CSA) are reported. The intrinsic metallic nature of conducting polyaniline can be observed from the positive temperature coefficient of resistivity in the temperature interval from 180 to 300 K. Signatures of hopping transport are observed below 180 K, indicative of marginal metallic behavior with disorder-induced localization at low temperatures. Resistivity ratios as low as 1:3 (300 to 1.2 K) are found. Analysis of the dependence of the resistivity on temperature and magnetic field indicates that the typical electronic localization length in PANI-CSA films is 100–150 Å. Thus the PANI-CSA is on the metal-insulator (*M-I*) boundary. A magnetic field (*H*) shifts mobility edge and causes the system to crossover from disordered metal to insulator: in zero field, $\rho(T) \propto T^{-\beta}$ where $\beta = 0.36$, consistent with transport in the critical region near the *M-I* boundary, whereas, in $H = 8$ T, $\rho(T) = \rho_0 \exp[(T_0/T)^{1/4}]$ indicating variable range hopping between localized states with mean localization length, $L_c(H = 8 \text{ T}) \approx 100$–140 Å.

INTRODUCTION

Polyaniline has emerged as one of the most promising conducting polymers;[1,2] PANI is environmentally stable, it exhibits relatively high conductivity, and it can be processed in both the insulating emeraldine base form[3] and in the conducting emeraldine salt form.[4] Recent progress has demonstrated that functionalized sulfonic acids can be used to protonate PANI and, simultaneously, to induce solubility of PANI in the conducting form in common nonpolar or weakly polar organic solvents.[5] The use of sulfonic acids with surfactant counterions, such as dodecylbenzene sulfonic acid (DBSA) and camphor sulfonic acid (CSA), results in relatively high electrical conductivities; values of 100–400 S/cm are routinely and reproducibly obtained from measurements on films (nonoriented) cast from solution.[5]

Although relatively high conductivity values have been reported for polyaniline doped with conventional protonic acids,[6] the conductivity of such materials is typically activated and decreases by several orders of magnitude as the temperature is lowered, in contrast to the behavior expected for a metal. This strong temperature dependence arises from a combination of mesoscale inhomogeneity ("metallic islands"[6]) and microscopic disorder (localization of the electronic wave functions)[7] both of which are indicative of the quality of the material. Thus, PANI has been characterized as a Fermi glass rather than as a true metal[7] or alternatively, as a collection of metallic islands separated by insulating barriers.[6]

The high conductivities obtained with PANI-CSA and PANI-DBSA imply that the sufactant counterions result in improved structural order on the molecular scale with fewer defects.[5] This was confirmed by measurements of the magnetic susceptibility;[8] PANI-CSA exhibits the temperature-independent Pauli-spin susceptibility expected for a metal, with a density of localized spins (Curie law behavior) that is lower than found in PANI with conventional counterions.[9] These improved materials, therefore, provide an opportunity to reexamine the temperature and magnetic-field dependences of the transport properties of PANI to look for the signatures of metallic behavior.

We summarize the results of measurements of the temperature dependence of the electrical properties of films of PANI-CSA. The intrinsic metallic nature of protonated PANI has been observed; the resistivity exhibits a positive temperature coefficient in the temperature interval from 180 to 300 K. Signatures of hopping transport are observed below 180 K, indicative of marginal metallic behavior with disorder-induced localization at low temperatures. Resistivity ratios as low as 1:3 (300 to 1.2 K) are found. From analysis of the dependence of the conductivity on temperature and magnetic field, we are able to estimate the typical electronic localization length in PANI-CSA films to be 100–200 Å.

EXPERIMENTAL DETAILS

PANI-CAS was prepared by mixing 1.092 g (0.012M) of emeraldine base with 1.394 g (0.006M) of ($\pm$)-10 camphor sulfonic acid using an agate mortar and pestle in a dry bag filled with nitrogen. The molar ratio of CSA to phenylnitrogen repeat unit was 0.5 in order to completely protonate the PANI to the emeraldine salt form. PANI-CSA is soluble in various organic solvents;[5] for this study, high-quality films were prepared by casting the material from solution metacresol.[10] Two types of films were prepared: from 2% and 4% (by weight) solutions of PANI-CSA in metacresol, denoted as PANI-CSA-2 and PANI-CSA-4, respectively. The solutions were prepared by adding an appropriate quantity of PANI-CSA to *m*-cresol (e.g., 1.0 g of PANI-CSA to 24 g of *m*-cresol to

yield a 3.9% solution); the mixture was then treated in an ultrasonic bath for 48 h and subsequently centrifuged. Most of the PANI-CSA complex dissolved to give a deep green solution; minor insoluble solids were removed by decanting. Free-standing PANI-CSA films were obtained by casting onto glass plates and subsequently drying in air for 24 h on a hot plate at 50 °C. Film thicknesses were typically 30–40 μm. Since the PANI-CSA was cast from solution, the PANI chains are neither chain extended nor chain aligned. The films are, therefore, in all respects iso-tropic.

Both PANI-CSA-2 and PANI-CSA-4 films are pro-tonated to the green emeraldine salt form with a nominal PANI:CSA ratio of 1:0.5. Because of the higher concen-tration of polymer, the 4% solutions are more viscous; apparently, the different rate of solvent evaporation dur-ing film formation either causes the PANI-CSA-2 and PANI-CSA-4 films to have slightly different protonation levels or causes a subtle change in the morphology of the resulting material. The results from PANI-CSA-2 and PANI-CSA-4 films are each reproducible (four indepen-dent samples of PANI-CSA-2 were measured and three independent samples of PANI-CSA-4 were measured). Although the transport properties are similar, the PANI-CSA-2 films appear to be of higher quality (and thus more nearly metallic) as judged by the temperature dependence of the resistivity.

Four-terminal dc resistivity and magnetoresistance measurements were carried out using a computer-controlled automated measuring system. Electrical con-tacts were made with conducting graphite adhesive. To avoid sample heating, the current source was adjusted at each temperature so that the power dissipated into the sample was less than 1 μW. The linearity was checked by measuring voltage versus current, and the resistivity was obtained from the slope of the straight line. Temperature (T) was measured with a calibrated platinum resistor (300 to 40 K) or a calibrated carbon-glass resistor (40 to 1.2 K) monitored by a temperature controller driven by the computer.

TEMPERATURE DEPENDENCE OF THE RESISTIVITY

The resistivities of PANI-CSA-2 and PANI-CSA-4 films are shown as a function of temperature in Fig. 1. The room-temperature values obtained for these two films were essentially identical, 280 S/cm. As shown in Fig. 1, the resistivity ratio $r = \rho(1.2$ K$)/\rho(300$ K$)$ is different for the two types of PANI-CSA films; $r \approx 3$ for PANI-CSA-2 films and $r \approx 12$ for PANI-CSA-4 films. Nevertheless, the $\rho(T)$ dependence is extremely weak in both cases; for example, even at the lowest temperatures the ratios $\rho(1.2$ K$)/\rho(4.2$ K$)$ for PANI-CSA-2 and PANI-CSA-4 films are only 1.4 and 2.5, respectively.

Over a limited temperature range below room tempera-ture, the resistivity of PANI-CSA has a positive tempera-ture coefficient ($d\rho/dT > 0$) consistent with metallic be-havior. As shown in the inset of Fig. 1, the positive tem-perature coefficient extends down to 180–190 K for PANI-CSA-2 and down to 220–230 K for PANI-CSA-4. In PANI-CSA-2 films, the resistivity decreases by about 10% between room temperature and the minimum near
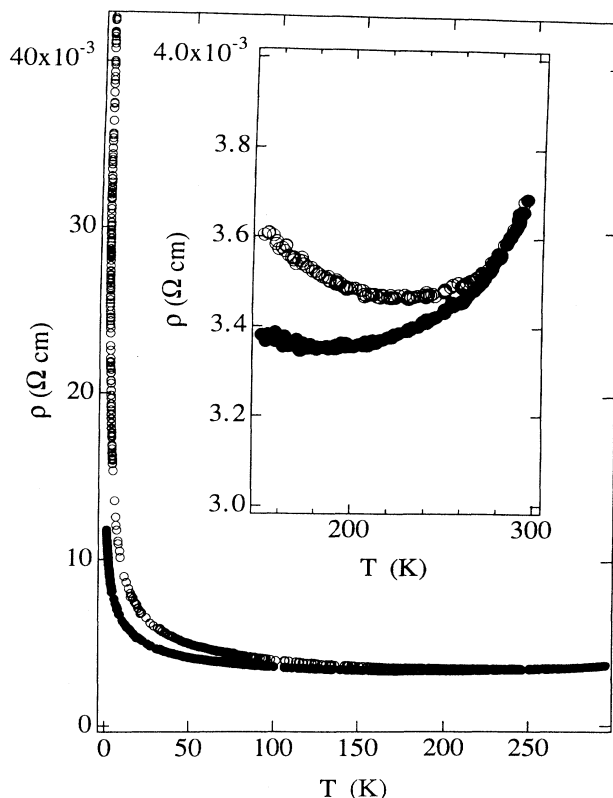

FIG. 1. Resistivity (ρ) vs temperature for PANI-CSA-2 (solid dots) and -4 (open dots). The inset shows the resistivity minima on an expanded scale.

180 K; in PANI-CSA-4 films the decrease is slightly smaller. We find excellent reproducibility with no hys-teresis on cycling the temperature (for example, from 300 to 1.2 K and back). The positive temperature coefficient is a general feature of PANI-CSA and was observed in all samples. This typically metallic characteristic has been seen previously in a conducting polymer only in the case of highly conducting polyacetylene.[11]

Based on the results of a series of conductivity, mag-netic susceptibility, and spin dynamics measurements (primarily on PANI protonated by exposure to HCl to form PANI-Cl), a granular-metal or "metallic island" model was proposed in which conducting segments of po-laronic metal form metallic regions surrounded by insu-lating barriers.[6,12−15] In such PANI-Cl samples, the resistivity increases by more than three orders of magni-tude when cooling to 30 K. The dependence observed in transport measurements.

$$\rho(T) = \rho_0 \exp[(T_0/T)^{1/n}] , \qquad (1)$$

with $n = 2$, was explained as arising either from the charging-energy-limited tunneling between metallic grains[16] or from a distribution of hopping energies due to variations in the effective conjugation length.[17]

Figure 2 compares $\sigma(T)$ versus T for PANI-CSA and PANI-Cl; the conductivity of PANI-CSA is higher and the temperature dependence is qualitatively different; the conductivity of the PANI-CSA-2 sample is nearly con-stant (see Fig. 1) while that of PANI-Cl drops by more
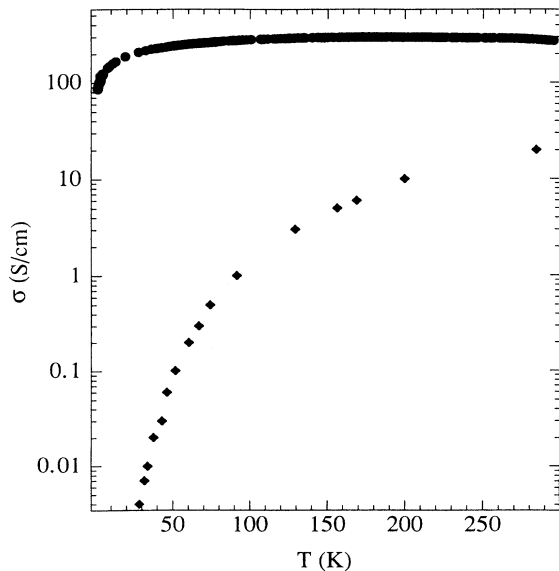
FIG. 2. Comparison of conductivity $\sigma(T)$ vs T for PANI-CSA-2 (solid dots; data from Fig. 1) and PANI-Cl (solid diamonds; data obtained from Ref. 6).

FIG. 3. Log resistivity vs log temperature for PANI-CSA-2: dots, $H = 0$, pluses, $H = 4$ T; and diamonds, $H = 8$ T. The solid line represents $\rho(T) \propto T^{-0.36}$ [see Eq. (5)]. Above 5 K, the $H = 4$ and $H = 8$ T data are not distinguishable from $H = 0$. The inset shows the resistivity vs magnetic field at 1.2 K for PANI-CSA-2.

than three orders of magnitude as the temperature is lowered.[6] Since $\rho(T)$ for PANI-CSA shows a much weaker temperature dependence, models involving relatively large scale inhomogeneity (such as "metallic islands," etc.) are not appropriate. The disorder in PANI-CSA is sufficiently small and the localization lengths are sufficiently large that the material is close to the metal-insulator boundary.

At temperatures below that of the resistivity minimum, the weak temperature dependence of PANI-CSA-2 samples cannot be fit to hopping transport expressions such as Eq. (1) with $n = 4,3,2$, etc. As shown in Fig. 3, a log-log plot of resistivity versus temperature is linear with slope β over the relatively wide range from 1.2 to 80 K; for PANI-CSA-2 samples, $\rho(T) = \rho_0 T^{-\beta}$, where $\beta = 0.36$. Similar power-law behavior has been observed for n-doped Ge in the metallic regime near the metal-insulator transition.[18] The inset of Fig. 3 shows the magnetic-field dependence (at low fields) of the resistivity at 1.2 K. The negative magnetoresistance in weak fields indicates that the mean localization length of the electronic wave functions is quite large, similar to that inferred from the negative magnetoresistance[19] in the variable-range hopping conduction in inorganic semiconductors which are doped to be near the metal-insulator transition. The negative magnetoresistance is also observed in PANI-CSA-4 samples.

Both the positive temperature coefficient of resistivity (at high temperatures) and the negative magnetoresistance in weak fields (at low temperatures), indicate that PANI-CSA is nearly metallic. Since there is a finite density of states at the Fermi energy (as inferred from the temperature-independent Pauli susceptibility)[6] the increase in resistivity at low temperatures results from disorder-induced localization; PANI-CSA is a Fermi
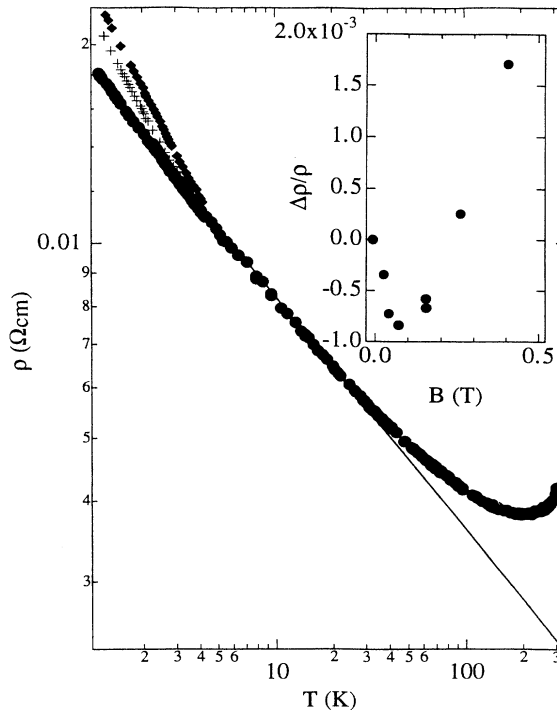
glass. The positive temperature coefficient above 200 K suggests the existence of a mobility edge very near the Fermi energy.

For PANI-CSA-4, the best fit to the low-temperature data is obtained from Eq. (1) with $n = 4$; i.e., variable-range hopping in three dimensions with[20,21]

$$T_0 = 16/k_B N(\varepsilon_F) L_{\text{loc}}^3 , \tag{2}$$

where k_B is the Boltzmann constant, $N(\varepsilon_F)$ is the density of states at the Fermi level, and L_{loc} is the localization length. The data are plotted as $\ln\rho$ versus $T^{-1/4}$ in Fig. 4; from the slope one obtains $T_0 = 200$ K. The mean hopping distance R_{hop} and the mean hopping energy difference between sites Δ_{hop} are given in terms of T_0 by the following expressions:[22]

$$R_{\text{hop}}/L_{\text{loc}} = \tfrac{3}{8}(T_0/T)^{1/4} , \tag{3a}$$

$$\Delta_{\text{hop}} = \tfrac{1}{4}k_B T (T_0/T)^{1/4} . \tag{3b}$$

The variable-range hopping theory is usually considered applicable when the wave functions are exponentially localized and when R_{hop} is considerably greater than the typical localization length. When T_0 is small, however, and the system is very near the metal-insulator boundary, the localized states extend over many molecular repeat units, and $R_{\text{hop}} \approx L_{\text{loc}}$ implying that hopping between nearest-neighbor localized states dominates. Thus, for
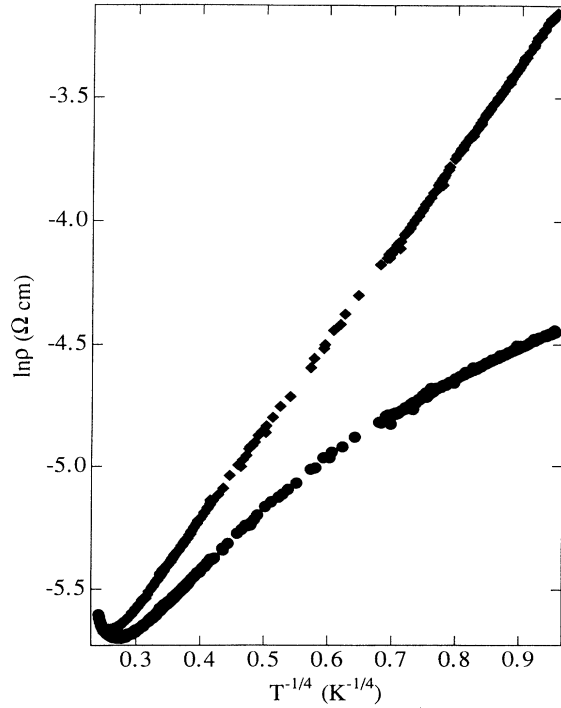
FIG. 4. Natural log of $\rho(T)$ vs $(T)^{-1/4}$ for PANI-CSA-2 (solid dots) and PANI-CSA-4 (solid diamonds).

$T_0 = 200$ K, one expects variable-range hopping to be valid for $T \ll 200$ K. Indeed, the PANI-CSA-4 data fall on a straight line in Fig. 4 only for $T < 100$ K. One expects an intermediate temperature interval in which the conductivity decreases as $\sigma = \sigma_c \exp[-|E_F - E_c|/k_B T]$ where $|E_F - E_c|$ is the energy between the Fermi energy (E_F) and the mobility edge (E_c), and σ_c is the conductivity at the mobility edge.[20] When the data from PANI-CSA-4 are replotted as $\ln \sigma$ versus T^{-1}, one finds an exponential dependence between about 100 and 180 K with $|E_F - E_c| \approx 30$ K and $\sigma_c \approx 340$ S/cm. As expected,[20] the value obtained for σ_c is close to that expected for the minimum metallic conductivity in three dimensions.[20]

For PANI-CSA, $N(\varepsilon_F)$ can be obtained from the magnitude of the temperature-independent Pauli contribution to the magnetic susceptibility—the data yield 1 state per eV per two rings[8]—using the approximate unit cell dimensions[23] of $a = 5.9$ Å, $b = 10$ Å, and $c = 7.2$ Å, $N(\varepsilon_F) \approx 2.4 \times 10^{21}$ states/eV cm^3. The value calculated from Eq. (2) for the localization length from this density of states is approximately 75 Å. The corresponding values are $R_{hop} = 70$ Å (at 100 K) and 215 Å (1.2 K); $\Delta_{hop} = 2.5 \times 10^{-3}$ eV (at 100 K) and 10^{-4} eV (at 1.2 K); see Eq. (3).

MAGNETIC-FIELD DEPENDENCE OF THE RESISTIVITY

The localization length can be independently estimated from the magnetic-field dependence of conductivity, using the following equation (applicable for hopping conduction)[24]
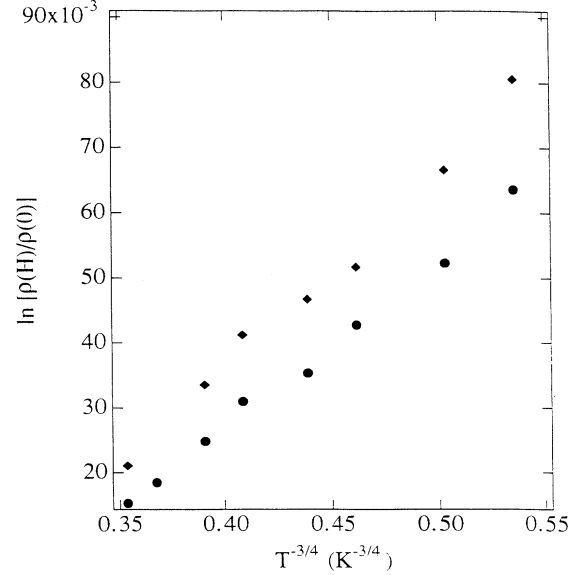

FIG. 5. Natural log of $[\rho(H)/\rho(0)]$ vs $(T)^{-3/4}$ at $H = 4$ T for PANI-CSA-2 (solid dots) and PANI-CSA-4 (solid diamonds).

$$\ln[\rho(H)/\rho(0)] = t(L_{loc}/L_H)^4(T_0/T)^{3/4} . \qquad (4)$$

where $t = (5/2016)$, $L_H = (c\hbar/eH)^{1/2}$ is the magnetic length, $\hbar$ is Planck's constant, c is the velocity of light, e is the charge of the electron, and H is the magnetic field. The data plotted as $\ln[\rho(H)/\rho(0)]$ versus $T^{-3/4}$ are plotted in Fig. 5 [with $\rho(H,T)$ measured at $H = 4$ T and at $H = 0$]. The value of L_H at 4 T is 128 Å. By knowing T_0 and the slope of $\ln[\rho(H)/\rho(0)]$ versus $T^{-3/4}$ one can solve for the localization length; for the PANI-CSA-4 samples, we find $L_{loc} = 160$ Å and $N(\varepsilon_F) = 10^{21}$ states per eV per cm^3, respectively. These values are in reasonable agreement with those directly inferred from T_0 and the density of states.

TRANSPORT AT THE METAL-INSULATOR BOUNDARY: MAGNETIC-FIELD-INDUCED CROSSOVER OF PANI-CSA-2 FROM DISORDERED METAL TO INSULATOR

In the Ioffe-Regel limit, disorder-induced scattering is sufficiently strong that the electronic mean free path approaches the electron's de Broglie wavelength; for stronger scattering, the wave functions become localized. In this limit of Anderson localization, a conductor which has a partially filled band for weak disorder (and thus would be a metal), becomes an insulator.[20] If the disorder is not large enough to cause localization throughout the band, the localized and extended states are separated at the mobility edge E_c.[20] In such a system, the metal-insulator $(M-I)$ transition is defined by the Fermi energy E_F, relative to E_c. If E_F is in the region of extended states, the conductivity remains finite as $T \to 0$ K; the system is a metal. If E_F is in the region of localized states, the system is an insulator in which the low-temperature transport is dominated by variable-range

hopping (VRH).[20]

The scaling theory of localization[25] confirmed the existence of the mobility edge, but with a continuous decrease of the conductivity to zero (rather than a discontinuous drop[20]) as E_F is moved through E_c. For a three-dimensional (3D) conductor in the metallic regime, but very close to the M-I transition (i.e., $\delta = [(E_F - E_c)/E_c] \ll 1$), the correlation length (L_c) is large and has a power-law dependence on δ, $L_c \approx a\delta^{1/\eta}$ where a is a microscopic length and η is the critical exponent.[26] In this critical region, Larkin and Khmelnitskii[26] found that the resistivity is not activated, but follows a power law as a function of the temperature (T),

$$\rho(T) \approx (e^2 p_F/\hbar^2)(k_B T/E_F)^{-1/\eta} , \qquad (5)$$

where p_F is the Fermi momentum, e is the electron charge, and $1 < \eta < 3$.

Khmelnitskii and Larkin[27] used scaling arguments to demonstrate that in the metallic region near the M-I transition, the mobility edge can be shifted by an external magnetic field. When the magnetic length,[24] $L_H = (\hbar c /eH)^{1/2}$, becomes comparable to L_c, the shift in E_c is proportional to $(L_H/L_c)^{1/\eta}$, where $\hbar$ is Planck's constant and c is the velocity of light. Because of this ability to shift E_c by an external magnetic field, one can envision a crossover from metallic behavior with power-law dependence for $\rho(T)$ in zero field to insulating behavior with variable-range hopping among localized states for $L_H/L_c < 1$. To our knowledge, such a crossover has not been previously observed.

At temperatures below that of the minimum in $\rho(T)$, the weak T dependence of PANI-CSA-2 cannot be fit to VRH expressions like $\rho(T) = \rho_0 \exp[(T_0/T)^{1/n}]$ with $n = 4$, 3, or 2. As shown in Fig. 6, a log-lot plot of $\rho(T)$ versus T (for $H = 0$) is linear; over the temperature range from 1.2 to 30 K, $\rho(T,0) = \rho_{0m}(T/T_{0m})^{-\beta}$, where ρ_{0m} and T_{0m} are constants, and $\beta = 0.36$. The sample-to-sample variation of the exponent correlates with the value for $\rho(300 \text{ K})$ and with the ratio $\rho(1.2 \text{ K})/\rho(300 \text{ K})$; samples with lower (higher) $\rho(300 \text{ K})$ and smaller (larger) $\rho(1.2 \text{ K})/\rho(300 \text{ K})$ give slightly smaller (larger) β; we find $\beta \approx 0.36 \pm 0.05$. The temperature range over which the dependence is a power law is wider for samples with smaller $|\beta|$.

Assuming the resistivity in zero magnetic field follows Eq. (5) with $\eta \sim (0.36)^{-1} = 2.77$,

$$\rho_{0m} \approx e^2 p_F/\hbar^2 \approx 2 \times 10^{-4} \ \Omega \text{ cm} , \qquad (6)$$

where we have used $p_F = \hbar k_F$, $k_F = \pi/2c$. Using the data in Fig. 6 and assuming $E_F \approx 1$ eV,[28] we find $\rho_{0m} \approx 6 \times 10^{-4} \ \Omega$ cm, in approximate agreement with the theoretical value [Eq. (6)].

The low-T data in Fig. 3 show a relatively large magnetoresistance, independent of whether the field is applied in the plane or perpendicular to the plane of the film. In high magnetic fields, the log-log plot of $\rho(T)$ versus T is not linear; for example, at $H = 8$ T, the $\rho(T,H)$ data in Fig. 6 do not fall on a straight line. The data of Fig. 3 are replotted in Fig. 6 as $\ln\rho(T)$ versus $T^{-1/4}$. For $H = 0$, the plot shows curvature (see also Fig. 4) consistent with
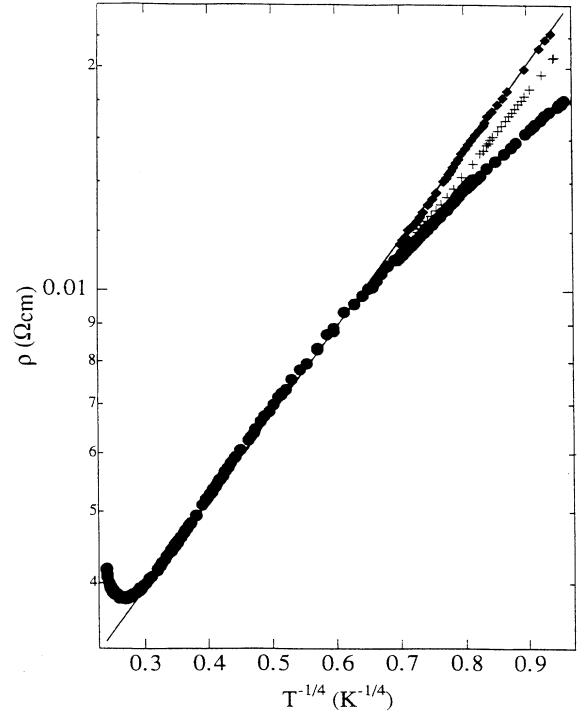

FIG. 6. $\ln\rho(T)$ vs $(T)^{-1/4}$ for PANI-CSA-2: dots, $H = 0$; pluses, $H = 4$ T; and diamonds, $H = 8$ T. The solid line represents VRH [Eq. (3)] with $T_0 = 56$ K. Above 5 K, the $H = 4$ and 8 T data are not distinguishable from $H = 0$.

the weaker dependence demonstrated in Fig. 3; i.e., $\rho(T)$ proportional to $T^{-0.36}$. In high magnetic fields, however, the $\ln\rho(T)$ versus $T^{-1/4}$ plot approaches straight-lint behavior. At 8 T,

$$\rho(T) = \rho_0 \exp[(T_0/T)^{1/4}] , \qquad (7)$$

indicative of variable-range hopping between *localized* states.

For VRH in 3D,[20] $T_0 = 16/k_B N(E_F)L_c^3$, where k_B is the Boltzmann constant. The slope of the $H = 8$ T data in Fig. 3 gives $T_0 = 56$ K. From the Pauli susceptibility, $N(E_F) \approx 1$ state per eV per two rings,[6,8,9] or $N(E_F) \approx 2.5 \times 10^{21}$ states/eV cm^3 (using the unit cell dimensions[29]). Substituting for $N(E_F)$ in the expression for T_0, we find $L_c \approx 112$ Å. Again, samples with lower (higher) $\rho(300 \text{ K})$ and smaller (larger) $\rho(1.2 \text{ K})/\rho(300 \text{ K})$ give slightly larger (smaller) L_c; we find $L_c \approx 100$–140 Å.

Although the origin of the magnetic-field-induced crossover is not understood in detail, the mobility edge can be shifted by an external magnetic field[27] when the magnetic length becomes comparable to the correlation length. The value of L_H at 8 T is approximately 90 Å, comparable to $L_c \approx 112$ Å as inferred from the slope of Fig. 6.

We have discussed the resistivity (versus T and H) in terms of transport in 3D. We note, however, that the intrinsic conductivity in a chain-extended and chain-oriented conducting polymer is anisotropic.[30] Since there is no significant chain orientation in the solution-cast

PANI-CSA films, the discussion in terms of 3D localization would appear to be justified. However, a more detailed analysis of disorder induced localization in polyaniline must take into account the intrinsically anisotropic transport (intrachain versus interchain).

INTRINSIC CONDUCTIVITY OF PANI-CSA

The large value for the mean localization length inferred from the low-temperature data suggests a qualitative explanation for the nonmonotonic temperature dependence. At low temperatures, the localized electronic wave functions extend over approximately 100–200 Å. As the temperature increases, phonons initially reduce the resistivity by delocalization of the electronic wave functions through phonon-assisted hopping and inelastic scattering. At still higher temperatures, phonon scattering causes the electron mean free path to become less than the mean localization length, and the resistivity increases, as in a metal. The crossover should occur when the inelastic mean free path $L_{\text{inelastic}}$ is comparable to the localization length, i.e., approximately $L_{\text{inelastic}} \approx 100$–$200$ Å. This implies an intrinsic conductivity parallel to the chain axis in an aligned sample of the following magnitude:

$$\sigma_{\text{int}} = Ne^2\tau/m = (Ne^2/\hbar k_F)L_{\text{inelastic}} , \qquad (8)$$

where N is the density of carriers and k_F is the Fermi wave number in the chain direction. Using $N \approx 2.5 \times 10^{21}$ cm^{-3} and $k_F \approx (\pi/2c)$ where $c \approx 7$ Å, we estimate $\sigma_{\text{int}} \approx 2.5 \times 10^4$ S/cm. In a nonoriented sample, the measured value would be reduced by the anisotropy. An alternative estimate can be obtained from the observed increase in resistivity in the region of the positive temperature coefficient; $\Delta\rho \sim 3 \times 10^{-4}$ Ω cm. This would imply $\sigma_{\text{int}} \sim 3 \times 10^3$ S/cm for a *nonoriented* sample; since the anisotropy would be expected to reduce the value in a nonoriented sample by about a factor 10–100,[30] the estimated value for $\sigma_{\parallel}$ (300 K) would be in excess of 3×10^4 S/cm. We conclude that for chain-oriented and chain-aligned PANI, the intrinsic conductivity along the chain axis at room temperature should be greater than 10^4 S/cm.

CONCLUSION

In conclusion, the magnitude of the resistivity of PANI-CSA is much smaller and the temperature dependence of the resistivity is much weaker than previously reported for protonated polyaniline containing conventional counterions (e.g., Cl$^-$). The metallic nature of PANI-CSA is observed in the transport from the increase in resistivity as the temperature is increased from 180 K to room temperature. The weak temperature dependence indicates that the use of surfactant counterions significantly improves the quality of the material; microscopic disorder has been reduced to the point of marginal metallic behavior with localization lengths at low temperatures of approximately 100–200 Å.

The power-law dependence of the resistivity, $\rho(T) \propto T^{-0.36}$, indicates that PANI-CSA is in the critical region of the metal-insulator transition. Application of an external magnetic field causes a crossover from the Larkin-Khmelnitskii power-law dependence of the disordered metal in the critical regime to variable-range hopping among localized states near the Fermi energy.

The counterion-induced processibility provides an opportunity to further improve the structural order to achieve chain-extended and chain-aligned PANI in which the elastic scattering is sufficiently weak to allow delocalization and true metallic behavior in three dimensions. In this limit, we estimate the room-temperature conductivity parallel to the chain direction to be greater than 10^4 S/cm.

[1]Y. Cao, P. Smith, and A. J. Heeger, in *Conjugated Polymeric Materials: Opportunities in Electronics, Optoelectronics and Molecular Electronics*, Vol. 82 of *NATO Advanced Study Institute, Series E: Applied Sciences*, edited by J. L. Bredas and R. R. Chance (Kluwer Academic, Dordrecht, 1990).

[2]A. G. MacDiarmid and A. J. Epstein, in *Science and Applications of Conducting Polymers*, edited by W. R. Salaneck, D. T. Clark, and E. J. Samuelson (Hilger, Bristol, 1991), p. 117.

[3]M. Angelopoulos, G. E. Asturias, S. P. Ermer, A. Ray, E. M. Scherr, and A. G. MacDiarmid, Mol. Cryst. Liq. Cryst. **160**, 151 (1988).

[4]A. Andereatta, Y. Cao. J. C. Chiang, P. Smith, and A. J. Heeger, Synth. Metals **26**, 383 (1988).

[5]Yong Cao, Paul Smith, and Alan J. Heeger, Synth. Met. **48**, 91 (1992).

[6]Z. H. Wang, E. M. Scherr, A. G. MacDiarmid, and A. J. Epstein Phys. Rev. B **45**, 4190 (1992); Z. H. Wang, C. Li, E. M. Scherr, A. G. MacDiarmid, and A. J. Epstein, Phys. Rev. Lett. **66**, 1745 (1991).

[7]F. Wudl, R. O. Angus, F. L. Lu, P. M. Allemand, D. J. Vachon, M. Nowak, Z. X. Liu, and A. J. Heeger, J. Am. Chem. Soc **109**, 3677 (1987).

[8]Y. Cao and A. J. Heeger, Synth. Met. **52**, 193 (1992).

[9]C. Fite, Y. Cao, and A. J. Heeger, Solid State Commun. **73**, 607 (1990).

[10]Yong Cao, Geroge M. Treacy, Paul Smith, and Alan J. Heeger, Appl. Phys. Lett. **60**, 1 (1992).

[11]A. B. Kaiser, Synth. Met. **45**, 183 (1991), and references therein.

[12]S. Sakkopoulos, E. Vitoratos, E. Dalas, G. Pandis, and D.

Tsamouras, J. Phys. Condens. Matter **4**, 2231 (1992).

[13]B. Lindberg, W. R. Salaneck, and I. Lundstrom, Synth. Met. **21**, 143 (1987).

[14]F. Zuo, M. Angelopoulos, A. G. MacDiarmid, and A. J. Epstein, Phys. Rev. B **36**, 3475 (1987).

[15]M. Nechtschein, F. Genoud, C. Menardo, K. Mizoguchui, J. P. Travers, and B. Villeret, Synth. Met. **29**, E211 (1989).

[16]Z. H. Wang, E. Ehrenfreund, A. Ray, A. G. MacDiarmid, and A. J. Epstein, Mol. Cryst. Liq. Crys. **189**, 263 (1990).

[17]L. W. Shacklette and R. H. Baughman, Mol. Cryst. Liq. Cryst. **189**, 193 (1990).

[18]A. N. Ionov, Fiz. Tekh. Poluprovodn. **14** 1287 (1980) [Sov. Phys. Semicond. **14**, 759 (1980)].

[19]A. N. Ionov and I. S. Shilmak, in *Hopping Conduction in Solids,* edited by M. Pollak and B. Shklovskii (North-Holland, Amsterdam, 1991), p. 397.

[20]N. F. Mott and E. Davis, *Electronic Processes in Noncrystalline Materials* (Clarendon, Oxford, 1979).

[21]S. Roth, in *Hopping Transport in Solids,* edited by M. Pollak and B. Shklovskii (North-Holland, Amsterdam, 1991), p. 377.

[22]R. Rosenbaum, Phys. Rev. B **44**, 3599 (1991).

[23]C. S. Yang, Y. Cao, P. Smith, and A. J. Heeger, Synth Met. (to be published).

[24]B. I. Shklvoskii and A. L. Efros, *Electronic Properties of Doped Semiconductors* (Springer-Verlag, Berlin, 1984), p. 212.

[25]E. Abrahams, P. W. Anderson, D. C. Licciardello, and T. V. Ramakrishnan, Phys. Rev. Lett. **42**, 673 (1979).

[26]A. I. Larkin and D. E. Khmelnitskii, Zh. Eksp. Teor. Fiz. **83**, 1140 (1982) [Sov. Phys. JETP **56**, 647 (1982)].

[27]D. E. Khmelnitskii and A. I. Larkin, Solid State Commun. **39**, 1069 (1981).

[28]S. Stafström, J. L. Bredas, A. J. Epstein, H. S. Woo, D. B. Tanner, W. S. Huang, and A. G. MacDiarmid, Phys. Rev. Lett. **59**, 1464 (1987).

[29]C. S. Yang (unpublished).

[30]Y. Cao, P. Smith, and A. J. Heeger, Polymer **32**, 1210 (1991).